Proceedings of 8th International Conference on Mechanical Engineering and Renewable Energy 2025
10-12 December, 2025, Chattogram, BANGLADESH
SciEn Conference Series: Engineering Vol. 4, 2026, pp 7-12 https://doi.org/10.38032/scse.2026.4.11

Evaluation of Evacuation Mapping in Industrial Fire Scenarios using CFD tools

Md. Kharshiduzzaman[1,], Musfiqul Azad[2], Syed Ishfaqul Hoque Rafsa[1], Mafrur Faharrim Khan[1], Redwanur Rashid [1], Md Foysal Mahmud [1]*

[1]Department of Mechanical and Production Engineering, Ahsanullah University of Science and Technology, Dhaka-1208, Bangladesh
[2]Prokausholee, Dhaka-1216, Bangladesh

ABSTRACT

Recently Bangladesh has witnessed a significant rise in industrial fire incidents. These structures often lack adequate fire safety systems causing smoke propagation during emergencies. This study evaluates the design of an industrial building comprising of 2 floors with an opening between them using Computational Fluid Dynamics (CFD) tool. The structure was simulated using PyroSim with two varying fire location. The environment was simulated for 12 minutes since ignition with a medium fire size. It was seen, within 3 minutes, smoke can engulf all exits of the storage room reducing visibility to dangerous level if fire source is in fabric storage. Comparative analyses show if fire is originated in production area, smoke migration is delayed offering better evacuation opportunities in ground floor. Toxic combustion product of cellulosic fuels like carbon monoxide (CO) cause intoxication and loss of consciousness whereas soot reduces the visibility. It is therefore important to predict the smoke conditions in a building during fire and find the ratio of ASET (Available Safety Egress Time) & RSET (Required Safety Egress Time). This study highlights importance of performance-based fire safety design, where perspective-based design falls short.

Keywords: ASET, RSET, Carbon Monoxide, Soot Density, CFD Tool, NIST, SFPE.

1. Introduction

In an industrial fire scenario, fire itself may be fatal but smoke inhalation can cause more fatalities in most cases. CO & soot are two common products of combustion of cellulosic fuels like cotton bale. Inhalation of CO causes lose on consciousness whereas soot decreases the visibility of the occupants ultimately delaying evacuation. The goal of this study is to systematically investigates the factors that affect the evacuation in industrial fire scenarios with 2 varying ignition source location. Factors like CO concentration, visibility and ASET were analyzed through simulations. For the simulation Pyrosim was used. The Large Eddy Simulation (LES) approach was selected along with the Smagorinsky sub grid scale model to capture turbulent smoke behavior exactly like FDS by NIST does. The core physics of PyroSim models matches FDS frameworks which have been validated. Inputs parameters were found from publications of NIST & SFPE.

2. Methodology

For the modeling the buoyant turbulent combustion of cotton bale, LES approach was used. LES resolves large-directly—making it especially suitable for simulating buoyancy-driven fire plumes, smoke layer formation, Smagorinsky LES model used in FDS extensively in literature, including forced/natural convection, smoke spread, and compartment fire tests.[1]

Pyrosim software code is used and validated worldwide for design calculations regarding prediction toxic gases spreading [9] and this research aims to analyses the spreading of smoke and how it affects evacuation time. In this research Pyrosim 2019 was used due to its capability of designing detailed geometry, defining specific material properties and assigning suitable boundary conditions. Smokeview was used to analyze visual ouputs of smoke distribution.

2.1. Governing Equations

Pyrosim solves numerically a modified version of the Navier-Stokes equations. It is suitable for low-speed, thermally-driven flow that focused on smoke and heat transport from fires similarly as FDS. [2] The equations are:

$$\frac{\partial \rho}{\partial t} + \nabla \rho u_i = 0 \tag{1}$$

$$\frac{\partial}{\partial t}(\rho u_i) + \nabla \cdot \rho u_i u_j + \nabla p = \rho f + \nabla \cdot \tau_{ij} \tag{2}$$

$$\frac{\partial}{\partial t}(\rho h) + \nabla \rho h u_i = \frac{Dp}{Dt} + \dot{q}''' - \nabla \cdot q + \emptyset \tag{3}$$

For perfect gas, we know

$$P = \rho R T \tag{4}$$

The equation of conservation of mass in terms of mass fraction of individual gaseous species can be expressed as,

$$\frac{\partial}{\partial t}(\rho Y_i) + \nabla \cdot \rho Y_i u = \nabla \cdot \rho D_i \nabla Y_i + \dot{m}_i''' \tag{5}$$

Where, u_i indicates velocity in i-direction and i =1, 2, 3, ρ indicates fluid density, f represents sum of external forces, τ_{ij} indicates shear stresses, p is pressure, h denoted as enthalpy, $\dot{q}'''$ is heat release rate per unit volume (HRRPUV), q is the heat transfer, Φ is any heat source, and T is the temperature. Y_i is the mass fraction. [8]

2.2 Large Eddy Simulation (LES) and Smagorinsky Sub-Grid Scale (SGS) Model

LES resolves large scales flow field solution allowing better fidelity whereas Reynolds Average Navier-Stokes Model (RANS model) provide only time averaged solution and oversimplify turbulent structures. on the other hand, Direct Numerical Simulations (DNS) tends to model the smallest scales of solution which increases computational cost. The continuity equation for incompressible flow in the filtered Navier-Stokes equation is:

$$\frac{\partial \bar{u}_i}{\partial x_i} = 0 \quad (6)$$

and the filtered Navier-Stokes equations,

$$\frac{\partial \bar{u}_i}{\partial t} + \frac{\partial}{\partial \varkappa_j}\left(\bar{u}_i \bar{u}_j\right) = -\frac{1}{\rho}\frac{\partial \bar{p}}{\partial \varkappa_i} + v\frac{\partial^2 \partial \bar{u}_i}{\partial \varkappa_j \partial \varkappa_j} - \frac{\partial}{\partial x_j}\tau_{ij} \quad (7)$$

$\bar{p}$ indicates the filtered pressure filed and τ_{ij} indicates the subgrid-scale stress tensor, τ_{ij} can be found by Eddy viscosity representation for small scale. [3]

$$\tau_{ij} = \frac{1}{3}\tau_{kk}\delta_{ij} = -2v_T\overline{\delta_{ij}} \quad (8)$$

δ_{ij} indicates the Kronecker's delta. In order to find τ_{ij}, the smagorinsky – Lilly subgrid scale SGS model is utilized. The Eddy viscosity can be modeled as:

$$v_T = (c_s \Delta g)^2\sqrt{2\overline{S_{ij}}\,\overline{S_{ij}}} = \left(c_s \Delta_g\right)^2 |s| \quad (9)$$

where $|s|$ is the magnitude of the strain-rate tensor and Cs denotes the Smagorinsky constant. Δg is the filter width that is calculated as:

$$\Delta_g = \left(\Delta_x \Delta_y \Delta_z\right)^{1/3} \quad (10)$$

2.3 Combustion Model and Radiation Transport

Mixture fraction model is the default combustion model in FDS. [4]. It is a conserved scalar quantity which defines the fraction of gas at a given point in the flow field that originated as fuel, as follows:

$$z = \frac{sY_F - \left(Y_{O_2} - Y_{O_2}^{\infty}\right)}{sY_F^I + Y_{O_2}^{\infty}};\, s = \frac{v_{O_2} W_{O_2}}{v_F W_F};\, v_F = 1 \quad (11)$$

Y indicates the mass fraction. Fuel is denoted by F and Oxygen by O_2. The fuel mass fraction in the fuel stream is denoted by Y_F^I . ∞ indicates free stream, far away from fire. The stoichiometric coefficient is ν. W stands for the gas molecular weight. The mixture fraction varies from Z=1 to Z=0. Where Z=1 indicates a region only containing fuel and Z=0 indicates a region where only ambient air is present. With the solution of the radiation transport equation for a non-scattering grey gas the radiative heat transfer is introduced in the model. The equation is solved using the Finite-Volume Method (FVM) [2].

2.4 Combustion Chemistry

Assuming complete combustion with stoichiometric AF ratio, combustion reaction of cellulose:

$$x\, C_6H_{10}0_5 + y\,(0_2 + 3.76N_2) \dashrightarrow a\, CO_2 + b\, H_20 + c\, N_2$$

In this study, the peak heat release rate (HRR) was calculated based on the complete combustion of cellulose ($C_6H_{10}O_5$), assuming full oxidation to CO_2 and H_2O. This assumption allowed for stoichiometric determination of oxygen demand, air-fuel ratio, and theoretical heat of combustion. Using empirical O_2-based heat values from SFPE charts, the HRR was derived by multiplying with the mass loss rate of the fuel. However, in real world fire scenario, combustion is hardly ever complete. While this method provides a thermodynamically consistent fire size, it does not explicitly account for incomplete combustion products such as CO and Soot. To account for this yield values CO and Soot was introduced in the simulation using yield parameters (kg/kg of fuel) as scaler values. These values control the rate of production of CO and soot based on local mass rate. These yield values are suggested by SFPE for various type materials. Incorporating these values help making the simulation more realistic and accounts for the inefficiency of realistic combustion. [5]. The balanced combustion reaction for cellulose assuming stoichiometric AF ratio (complete combustion) is:

$$6.1728\, C_6H_{10}0_5 + 37.0368\,(0_2 + 3.76N_2) \dashrightarrow 37.0368\, CO_2 + 30.8643\, h_20 + 139.2547\, N_2$$

Now based on the values of Table 5.3 [5] for 6.1728 mol or 1 kg of $C_6H_{10}0_5$ Heat of Combustion is calculated to be: $\triangle H_c$= (37.0368*32) g * (13.59) KJ/g = 16106.56 kJ/kg

Again, from the weight of 1kg cellulose using values form table 5.3 [5] the values of Heat of Combustion were found: $\triangle H_c$=16.09 kJ/kg * 1000g = 16090 kJ/kg

So, Heat Release Rate (HRR) = $\dot{m}_{\text{fuel}}$ * $\triangle H_c$ = 0.315 kg/s * 16106.56kJ/kg = 5073.39 kW For this study the combustible materials (cotton bale) total surface area was 20 m^2. So, Heat Release Rate Per Unit Area is found to be:

$$\text{HRRPUA} = \frac{5073.39\ kW}{20\ \text{m2}} = 253.66\ \text{kW/m}^2$$

2.5 Building Description and Computational Mesh

The studied model is an existing 2-story industrial building shown in Fig 1(a) is about with overall plan dimensions of about 96×96 m^2. The overall height is about 11m. The ground floor height from the floor is 3.514m and the first-floor height from the floor is 3.922m. A rectangular opening at the center of the building exists which is of (47.60×41.85)m^2 shown in fig 1(b). The governing equations were approximated on a rectilinear mesh (grid). The computational mesh containing 197×172×45 cells was used. The cells were almost cubic with dimensions of (0.888×0.889×0.888) m^3. Figure 1(c) illustrate the cells of the computational mesh. The cell size was intended to keep smaller than the characteristic fire diameter (D^*) which was calculated using this equation form NIST special publication 1018. [6]

$$\mathbf{D}^* = \left(\frac{\dot{Q}}{\rho_\infty\, c_p\, T_\infty \sqrt{g}}\right)^{2/5}$$

$\rho_\infty = 1.2\ kg/m^3$, c_p=1.006 kj/kg. k,T_∞= 308k, $\dot{Q}$=5073.56 kw

Here density, specific heat of air, temperature was considered for ambient conditions. The value of characteristic fire diameter was found to be 1.807m. The mesh size was kept half of this value as mentioned earlier.

Though smaller values could improve the overall results of the simulation, this value was chosen for limited computational power availability. As can be seen in Fig. 1(c), the computational domain was extended 27 m above the maximum roof height and 20 m on each side to facilitate the smoke exit through various openings. Several devices were placed in the egress route throughout the building to measure the CO concentration and soot visibility. Their positions are shown in fig 1(a) and fig 1(b).

Fig. 1(a) Ground Floor layout & device locations

The device which measures CO concentrations are represented as DC and visibility measuring devices are represented as DV in table 1 and table 2 respectively. Where 1,2,3,4 are the locations in fabric storage, ground floor and 21,22,23,24,25,26,27,28 are locations on first floor.

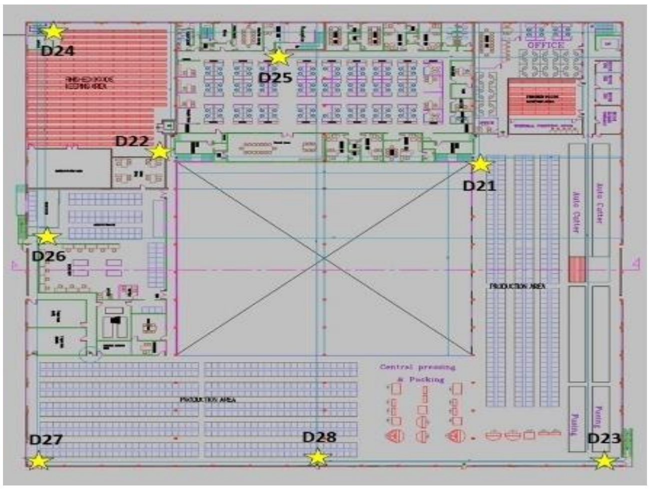

Fig. 1(b) First floor layout and device locations

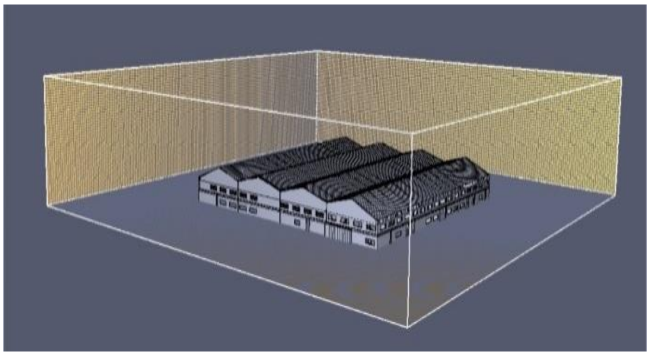

Fig. 1(c) Computational Domain

2.6 Boundary Conditions

No-penetration and no-slip conditions are applied on the solid surfaces. All the exhaust fans are assigned no flow boundary conditions. All doors are considered 100% open. All solid-surfaces are assigned noncombustible boundary conditions, Imperical co relations were used to model heat and mass transfer to and from solid surfaces. [7] The normal temperature (without fire) in the building was considered as 35°C. Energy released by the combustion of cotton bale was assigned 16090Kj/kg.[7]. t^2 fire growth model was used with peak time 300seconds for simulating medium fire. Thermal boundary condition of the burning object was assigned adiabatic. Relative humidity in the facility was considered 40% and outside temperature was Assumed to be same as inside. The ambient pressure was set to 101325 kpa. The initial oxygen and carbon dioxide mass fraction was set to 0.2324kg/kg and $5.9x10^{-4}$ kg/kg respectively. Carbon monoxide yield and soot yield of the cellulosic fuel is considered to 0.02 and 0.1 SFPE Handbook of Fire Protection Engineering provided charts for these values. The value of critical flame temperature of cellulosic fuel like compressed cotton can also found from the chapter 66 (fire chemistry) of this book. The critical flame temperature was set to 1300 ºC for the simulation and total of 12 minutes simulation was run [5]. The heat release rate per unit area was set to 250 kW/m^2.

3. Results and Discussion

In this study carbon monoxide concentration above 30ppm and visibility below 10m was considered as critical parameter. Fire was initiated on two different locations. Location F1 indicates fire in fabric storage & Location F2 indicates the fire in production area at the center of the building. Both fire source was placed in ground floor. The whole system was simulated for 720seconds. Fig 2(a) indicated the HRR curve from simulation result for the studied fire scenarios. From the curve it is seen that the peak HRR was 5073 kW which was previously calculated in section 2.4 and it is also seen that the peak HRR was reached at time 300seconds.

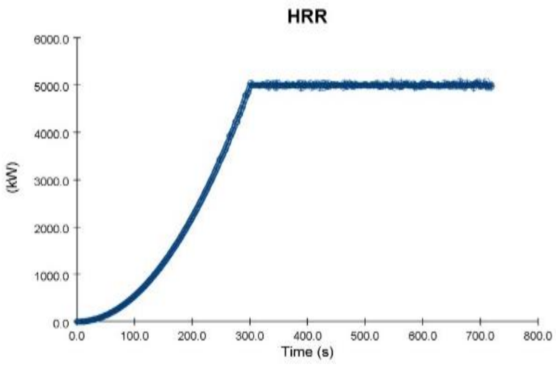

Fig. 2(a) HRR Curve of 5MW Fire

Figure 2(b) illustrates slice contours of the fabric storage room at 1.7m height from the ground floor when fire is initiated in case F1. It can be seen that within 183seconds majority of the fabric storage room is engulfed in smoke and the CO concentration has increased above $3e^{-05}$ mol/mol or 30ppm which is the dangerous limit in the study.

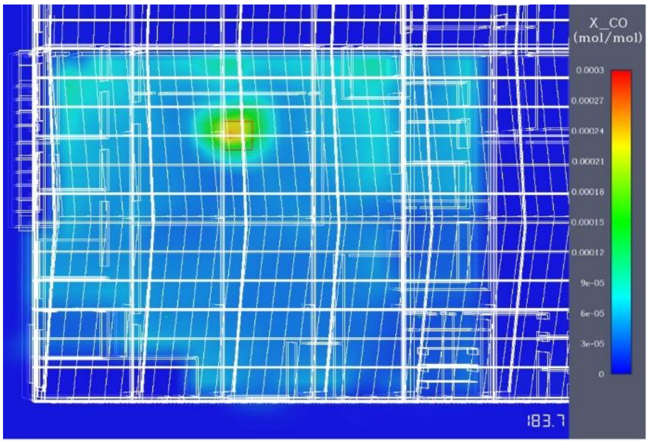

Fig. 2(b) Slice at 1.7m above the ground floor height of CO Concentration (case F1)

Fig 2(c) illustrates concentration of CO and it indicates at the maximum time of the simulation which is 720seconds, the concentration has increased to $4e^{-07}$ mol/mol or 0.4ppm at height 1.7m above first floor. This value is well below 30ppm. So, the conditions of evacuation for the occupants remains tenable throughout the fire scenario in case F2.

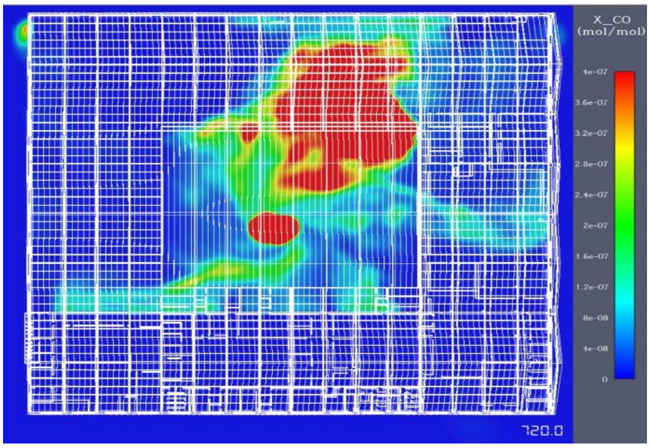

Fig. 2(c) Slice at 1.7m above the ground floor height of CO Concentration (case F2)

Fig 2(d) illustrates the slice contour of visibility at height 1.7m above first floor in case F1. It can be seen from the contour that visibility at first floor remains well above 10m until 620second since the ignition. The dangerous limits for visibility in this study is considered less than 10m.

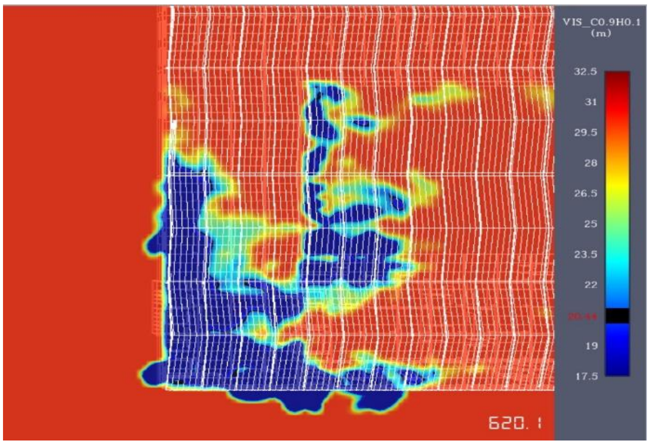

Fig. 2(d) Slice at 1.7m above the first floor height of visibility (case F1)

Fig 2(e) illustrates the slice contour of visibility at height 1.7m above first floor in case F2. It can be seen from the contour that visibility has dangerously dropped below 8m within 500seconds at almost every place of first floor.

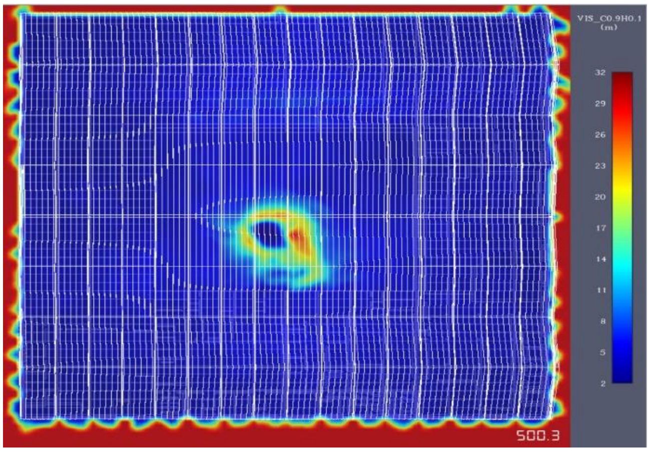

Fig. 2(e) Slice at 1.7m above the first floor height of visibility (case F2)

Table 1 indicates the values of CO concentration in ppm at the locations of all devices as previously discussed in fig 1(a) and in fig 1(b). The devices named as DC measures CO concentration. Comparison for both case F1 and F2 are shown in the table. It can be seen from the table that the CO concentration in locations of ground floor did not increase rather remained unaffected in case F2(indicated in blue) However, in case F1 all of them reached dangerous limit within 391 seconds. (Indicated in red).
Table 2 indicates the values of visibility in meter at the locations of all devices as previously discussed in fig 1(a) and in fig 1(b). The devices named DV measures visibility. Comparison for both case F1 and F2 are shown in the table. It can be seen that from the table, the devices which are placed in ground floor are unaffected in case F2(indicated in blue). However, the same locations are highly affected in case F1 (indicated in red). In case F2 most of the areas of the first floor are dangerously affected in very short time.

Table 1 Measured Values of devices for CO concentration (ppm)

Device	Time F1 (sec)	CaseF1 (ppm)	Time F2 (sec)	Case F2 (ppm)
DC1	183	30>	720	$1.6e^{-05}$
DC2	391	30>	720	$7e^{-07}$
DC3	204	30>	720	0.19
DC4	144	30>	720	0.0158
DC21	720	5.6	551	30>
DC22	720	1.62	677	30>
DC23	720	0	549	30>
DC24	720	0.31	506	30>
DC25	720	2.9	645	30>
DC26	720	1.13	447	30>
DC27	720	0	613	30>
DC28	720	0	720	22

Table 2 Measured Values of devices for Visibility (m)

Device	Time F1 (sec)	CaseF1 (m)	Time F2 (sec)	Case F2 (m)
DV1	143	<10	720	30
DV2	291	<10	720	30
DV3	137	<10	720	30
DV4	85	<10	720	30
DV21	720	10	237	<10
DV22	720	30	272	<10
DV23	720	30	332	<10
DV24	720	30	230	<10
DV25	720	20.7	296	<10
DV26	720	30	**201**	<10
DV27	720	30	324	<10
DV28	720	30	422	<10

It is notable in figure 1(a) and the tables that there are no devices placed outside the fabric storage compartment in ground floor. The reason is, through trial and error it was seen that in case F1 the smoke does not propagate out of the compartment within the total simulation time (720 seconds) and in case F2 the whole ground floor is very slightly affected by the smoke.

4. Conclusion

From the contours and tables, it can be seen that within 3minutes both the CO concentration and visibilities cross dangerous limit in the whole fabric storage room. It can also be clearly seen in case F1 that most of the areas in ground floor and first floor are unaffected or slightly affected by smoke though the fabric storage room itself is highly affected (DC 1,2,3,4). This phenomenon is due to exit of smoke through the windows and doors of the fabric storage room. The smoke exits out of the building through these opening rather than propagating to other compartments of the building. So, it is safe to say that the fabric storage room is well ventilated. On the other hand, within 500 seconds the complete visibilities at second floor dangerously falls below 8m hindering evacuation (fig2.e). The most critical position for safe evacuation for case F2 is V26 where visibilities fall below 10m in 201 seconds. However, in this case most of the areas of ground floor remains slightly affected or completely unaffected by smoke. This phenomenon is due to the uprise of smoke through the opening between floors and accumulation of smoke in the first floor. In these analyses the time represented in tables gives ideas about ASET in realistic fire scenarios. From the table its clear that if the combustible materials are kept in fabric storage room and a fire scenario occurs, most of the occupants in the buildings will be having enough time available to evacuate safely. But the situation in fabric storage compartment will be different. The occupants there will have to evacuate within 183 seconds otherwise serious accident can occur. In case F2 the occupants in ground floor will have enough time to evacuate but the occupants in first floor will have to evacuate within 201 seconds to be safe.

Along with the traditional perspective-based design, it's safe to further evaluate the design though performance-based approach. This helps ensuring if the design of the building is safe for the purpose it is intended to use for and give realistic ideas on how the structure performs in hazardous environment. This approach helps to seek out any existing design flaw before constructions.

References

[1] McGrattan, K., Hostikka, S., Floyd, J., Baum, H., Rehm, R., Mell, W. and McDermott, R. (2010) *Fire Dynamics Simulator (Version 5): Technical Reference Guide – Volume 1: Mathematical Model*. NIST Special Publication 1018-5. Gaithersburg, MD: National Institute of Standards and Technology.

[2] Smardz, P. (2006) *Validation of Fire Dynamics Simulator (FDS) for forced and natural convection flows*. MSc thesis. Department of Fire Safety Engineering, University of Ulster.

[3] Leonard, A. (1974) 'Energy cascade in large-eddy simulations of turbulent fluid flows', *Advances in Geophysics*, 18, pp. 237–248.

[4] McGrattan, K., Hostikka, S., Floyd, J., Baum, H., Rehm, R., Mell, W. and McDermott, R. (2010) *Fire Dynamics Simulator (Version 5): Technical Reference Guide – Volume 1: Mathematical Model*. NIST Special Publication 1018-5. Gaithersburg, MD: National Institute of Standards and Technology.

[5] Hurley, M.J. (ed.) (2016) *SFPE Handbook of Fire Protection Engineering*. 5th edn. Cham, Switzerland: Springer.

[6] National Institute of Standards and Technology (n.d.) *NIST Special Publication 1018*. Gaithersburg, MD: National Institute of Standards and Technology.

[7] McGrattan, K. (2006) Fire Dynamics Simulator (Version 4): Technical Reference Guide. NIST Special Publication 1018. Gaithersburg, MD: National Institute of Standards and Technology.

[8] Kashef, A., Bénichou, N., Lougheed, G. and Debs, A. (n.d.) 'Prediction of smoke propagation in a big multi-story building using Fire Dynamics Simulator (FDS)', American Journal of Energy Engineering. Science Publishing Group.

[9] Kallianiotis, A., Papakonstantinou, D., Tolias, I.C. and Benardos, A. (2021) 'Evaluation of fire smoke control in underground space', *Underground Space*, 7(2), pp. 295–310.

Nomenclature

Symbol	*Meaning*	*Unit*
ρ	Density	Kg/m^3
u	Velocity	m/s
f	External Force	N
τ	Shear Stress	Pa
t	Time	Sec
q	Heat Flux	W/m^2
$\dot{m}$	Mass Flow Rate	kg/s
h	Enthalpy	J
$\dot{q}'''$	Heat Release Rate per	
	Unit Volume	kW/m^2
Y	(HRRPUV)	
$\|s\|$	Mass Fraction	
C_s	Strain Rate Tensor	
v	Smagorinsky Constant	
	Stoichiometric	
Z	Coefficient	
HRRPUA	Mixture Fraction	kW/m^2
	Heat Release Rate per	
D^*	Unit Area	
	Characteristic Fire	
$\dot{Q}$	Diameter	kW
c_p	Power	kJ/kg
	Specific Heat of Air	